

Phase Diagrams for the Stability of the $\nu = 1/2$ Fractional Quantum Hall Effect in Wide GaAs Quantum Wells

J. Shabani, Yang Liu, M. Shayegan, L. N. Pfeiffer, K. W. West, and K. W. Baldwin
Department of Electrical Engineering, Princeton University, Princeton, NJ 08544, USA
 (Dated: March 18, 2019)

We report an experimental investigation of the unique fractional quantum Hall effect (FQHE) at the even-denominator Landau level filling factor $\nu = 1/2$ in very high quality wide GaAs quantum wells, and at very high magnetic fields up to 35 T. The quasi-two-dimensional electron systems we study are confined to GaAs quantum wells with widths W ranging from 44 to 96 nm, and have bilayer-like, symmetric charge distributions and variable densities in the range of $\simeq 4 \times 10^{11}$ to $\simeq 4 \times 10^{10}$ cm $^{-2}$. We present several experimental phase diagrams for the stability of the $\nu = 1/2$ FQHE in these quantum wells. First, for a given W , the $1/2$ FQHE is stable in a limited range of intermediate densities; it makes a transition to a compressible phase at low densities and to an insulating phase at high densities. The densities at which the $\nu = 1/2$ FQHE is stable are larger for narrower quantum wells. Second, we present a plot of the symmetric-to-antisymmetric subband separation (Δ_{SAS}), which characterizes the inter-layer tunneling, vs density for various W . This plot reveals that Δ_{SAS} at the boundary between the compressible and FQHE phases increases linearly with density. Finally, we summarize the experimental data in a diagram that takes into account the relative strengths of the inter-layer and intra-layer Coulomb interactions and Δ_{SAS} . We conclude that, consistent with the conclusions of previous studies, the $\nu = 1/2$ FQHE observed in wide GaAs quantum wells with symmetric charge distribution is likely a two-component state.

INTRODUCTION

The fractional quantum Hall effect (FQHE) [1] is predominantly seen in high-quality two-dimensional (2D) electron systems in the lowest ($N = 0$) Landau level at odd-denominator fillings ν [2]. In the first, excited ($N = 1$) Landau level, a FQHE exists at the *even-denominator* filling $\nu = 5/2$ [3, 4]. This enigmatic FQHE has become the focus of considerable theoretical and experimental attention, partly because of its potential application in topological quantum computing [5]. Despite numerous experimental efforts during the past two decades, however, a thorough understanding of its origin remains elusive. In particular, it is yet not known whether or not the spin degree of freedom is necessary to stabilize this state. If yes, then the $5/2$ FQHE state could be described by a two-component, Halperin-Laughlin (Ψ_{331}) wavefunction [6]. But if the $5/2$ FQHE is stable in a fully spin-polarized 2D electron system, then it is likely to be the one-component, Moore-Read (Pfaffian) state [7]. The latter is of enormous interest as it is expected to obey non-Abelian statistics and have use in topological quantum computing [5].

The possibility of an even-denominator FQHE in the *lowest* Landau level, e.g. at $\nu = 1/2$, has been theoretically discussed in numerous publications [6–20]. Experimentally, FQHE states at $\nu = 1/2$ have been seen in electron systems confined to either double [21], or wide [22–31] GaAs quantum well (QW) systems; a $\nu = 1/4$ was also observed recently in wide QWs [29–31]. In a double QW with negligible inter-layer tunneling but comparable inter-layer and intra-layer Coulomb interactions, it is generally accepted that the $\nu = 1/2$ FQHE is stabi-

lized by the additional (layer) degree of freedom, and is described by the two-component, Ψ_{331} state [8–12, 14–20]; in this case the components are the layer indices. However, the situation is more subtle for the case of electrons in a single, wide QW where the electron-electron repulsion lifts the potential energy near the well center and creates an effective barrier [22–32]. Although the system can have a “bilayer-like” charge distribution at sufficiently high densities, the inter-layer tunneling, quantified by the symmetric-to-antisymmetric subband separation (Δ_{SAS}), can be substantial. Moreover, in a QW of with a fixed well-width, the magnitude of Δ_{SAS} can be tuned from small to large values by decreasing the electron density in the QW while keeping the total charge distribution symmetric (“balanced”). When Δ_{SAS} is negligible compared to the intra-layer Coulomb energy ($e^2/4\pi\epsilon l_B$) then, similar to the double-QW system, Ψ_{331} is the likely ground state if a $\nu = 1/2$ FQHE is observed ($l_B = \sqrt{\hbar}/eB$ is the magnetic length and ϵ is the dielectric constant). If Δ_{SAS} is a significant fraction of $e^2/4\pi\epsilon l_B$, however, then it is likely that the $\nu = 1/2$ FQHE state is a one-component, Pfaffian state [13].

Here we present results of our extensive experimental study of the $\nu = 1/2$ FQHE in very high quality, wide GaAs QWs with well widths (W) ranging from 44 to 96 nm and tunable densities (n) in the range of $\simeq 4 \times 10^{11}$ to $\simeq 4 \times 10^{10}$ cm $^{-2}$. Our data, taken at low temperatures and very high perpendicular magnetic fields (B up to 35 T) allow us to determine the most comprehensive set of experimental conditions for the stability of the $\nu = 1/2$ FQHE in wide GaAs QWs. We present our data in several experimental phase diagrams, including a d/l_B vs $\Delta_{SAS}/(e^2/4\pi\epsilon l_B)$ diagram; d/l_B is the ratio of the inter-layer distance (d) and the mag-

netic length, and is a measure of the relative strengths the intra-layer ($e^2/4\pi\epsilon l_B$) and inter-layer ($e^2/4\pi\epsilon d$) interactions. We conclude that, consistent with the conclusions of previous experimental [24, 25, 30] and theoretical [14, 18, 19] studies, the $\nu = 1/2$ FQHE observed in wide GaAs QWs with symmetric charge distribution is likely a two-component state. We also compare our d/l_B vs $\Delta_{SAS}/(e^2/4\pi\epsilon l_B)$ phase diagram to a recently calculated diagram [19]. We find that there is an overall qualitative agreement, although there are significant quantitative discrepancies between the experimental and theoretical phase diagrams.

Our samples were grown by molecular beam epitaxy and each consists of a GaAs QW bounded on both sides by undoped $\text{Al}_x\text{Ga}_{1-x}\text{As}$ barrier layers ($x \simeq 0.24$ to 0.30) and Si δ -doped layers. The well widths of these samples range from 44 to 96 nm, but the focus of our work is on narrower QWs ($W < 70$ nm) where Δ_{SAS} is large. These narrower QW samples typically have low-temperature mobilities of 250 to 600 m^2/Vs and the Al composition in their barriers is $x \simeq 0.24$. The wider QW samples used in older studies [22–25] had mobilities of $\simeq 100$ m^2/Vs and their barriers had $x \simeq 0.30$. All the samples had a van der Pauw geometry, an approximately 3 mm \times 3 mm square shape, and were fitted with an evaporated Ti/Au front-gate and a Ga or an In back-gate to change the 2D density while keeping the charge distribution in the well symmetric. We carried out measurements in dilution refrigerators with base temperatures of $\simeq 30$ mK, housed in either a 16 T superconducting magnet or a 35 T resistive magnet.

Most of the samples used in our study were cut from GaAs wafers which were not rotated during the epitaxial growth. This resulted in a non-uniformity of the growth rate across the wafer surface and an uncertainty in the QW width. To determine the QW width more accurately, we carefully measured and analyzed the low-field Shubnikov-de Haas oscillations in each sample to obtain Δ_{SAS} as a function of n . We also performed calculations of the charge distribution and the QW's potential and energy levels by solving Schroedinger and Poisson's equations self-consistently (at zero magnetic field) while treating the QW width W as an adjustable parameter. We then compared the measured Δ_{SAS} vs n data to the calculations using W as a fitting parameter. The values of W we quote here are from such fits, and have an estimated accuracy of about $\pm 5\%$; they also agree with the nominal QW widths based on the epitaxial growth rates to within about $\pm 10\%$.

We first briefly describe the electron system confined to a modulation-doped wide QW. When electrons at very low density are placed in such a QW, they occupy the lowest electric subband and have a single-layer-like (but rather thick in the growth direction) charge distribution. As more electrons are added to the well while keeping the charge distribution symmetric, their electrostatic re-

pulsion forces them to pile up near the QW boundaries and the electron charge distribution appears increasingly bilayer-like [22–32]. At high n the electrons typically occupy the lowest two, symmetric and antisymmetric electric subbands; these are separated in energy by Δ_{SAS} , which for a bilayer system can be considered as the inter-layer tunneling energy. An example of the potential energy and the charge distribution in such a system is given in Fig. 1 inset where we show the results of our self-consistent calculations for $n = 3.42 \times 10^{11}$ cm^{-2} electrons symmetrically distributed in a 47-nm-wide QW.

A crucial property of the electron system in a wide QW is that both Δ_{SAS} and d (the inter-layer separation, see Fig. 1 inset), which characterize the coupling between the layers, depend on density: Increasing the density makes d larger and Δ_{SAS} smaller so that the system can essentially be tuned from a (thick) single-layer-like electron system at low density to a bilayer one by increasing the density [22–32]. This evolution with density plays a decisive role in the properties of the correlated electron states in the system [22–32]. At low densities, when Δ_{SAS} is large, the electron system exhibits odd-denominator FQHE characteristic of a standard, single-layer sample. In particular, at $\nu = 1/2$ the electron system is compressible and there is no FQHE. At very high densities, it shows an insulating phase near $\nu = 1/2$, which likely signals the formation of a bilayer Wigner crystal [26]. And eventually, at the highest densities, Δ_{SAS} becomes small and the system is very much bilayer-like; it typically exhibits FQHE at odd-denominator fillings which have *even numerators*, consistent with the presence of two layers in parallel. In the intermediate density regime, on the other hand, a FQHE is seen at $\nu = 1/2$ in the highest quality samples. This FQHE, and its transition into a compressible state as the density is lowered, are the subjects of our study presented here.

Experimentally, we control both the density and the charge distribution symmetry in our samples via front- and back-side gates, and by measuring the densities of the two occupied electric subbands from Fourier transforms of the low-field Shubnikov-de Haas magnetoresistance oscillations. These Fourier transforms typically exhibit two peaks whose frequencies are directly proportional to the subband densities. By carefully monitoring the evolution of these frequencies as a function of density and, at a fixed density, as a function of the values of the back and front gate biases, we can determine and tune the symmetry of the charge distribution [24–28, 30, 31]. Note that Δ_{SAS} is directly proportional to the difference between the subband densities and, for a fixed density in the QW, is smallest when the total charge distribution in the QW is symmetric. The data presented here were all taken on wide QWs with symmetric (“balanced”) charge distributions. Also, all the quoted values of Δ_{SAS} are from the measured Shubnikov-de Haas oscillation frequencies.

Figure 1 provides an example of the longitudinal (R_{xx})

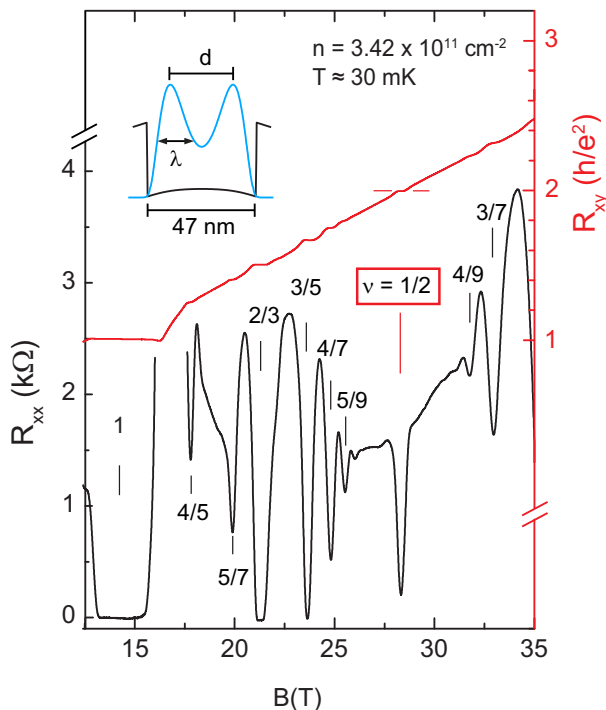


FIG. 1. (color online) Longitudinal (R_{xx}) and Hall (R_{xy}) resistance data for a 47-nm-wide QW at a density of $3.42 \times 10^{11} \text{ cm}^{-2}$. The inset shows the electron distribution (blue curve) and potential energy (black curve) calculated self-consistently at zero magnetic field.

and Hall (R_{xy}) resistance traces at high magnetic fields for a 47-nm-wide QW at a density of $3.42 \times 10^{11} \text{ cm}^{-2}$. R_{xx} minima are observed at numerous Landau level fillings such as $\nu = 2/3, 3/5, 4/7, 5/9$ and $6/11$, attesting to the very high quality of the sample. These odd-denominator FQHE states and their relative strengths resemble those seen in standard, single-layer, 2D electrons confined to a high quality GaAs QWs. Of particular interest here is of course the strong FQHE at $\nu = 1/2$ as evidenced by a deep R_{xx} minimum and a well-developed R_{xy} plateau quantized at $2h/e^2$. This FQHE has no counterpart in standard 2D electrons systems in narrow QWs. The charge distribution and potential for this QW at $n = 3.42 \times 10^{11} \text{ cm}^{-2}$, calculated self-consistently (at $B = 0$), are also shown in Fig. 1 inset. The charge distribution is bilayer-like, with d denoting the inter-layer distance and λ the full-width-at-half-maximum of the charge distribution in each "layer".

In Fig. 2 we show the density dependence of the R_{xx} traces for the same 47-nm-wide QW sample as in Fig. 1. The bottom x -axis used in Fig. 2 is the inverse filling factor in order to normalize the magnetic field for the different densities. At the lowest density (bottom trace) the FQHE states are very similar to those seen in the standard, narrow 2D electron systems; more precisely, they are all at odd-denominator fillings and there is no

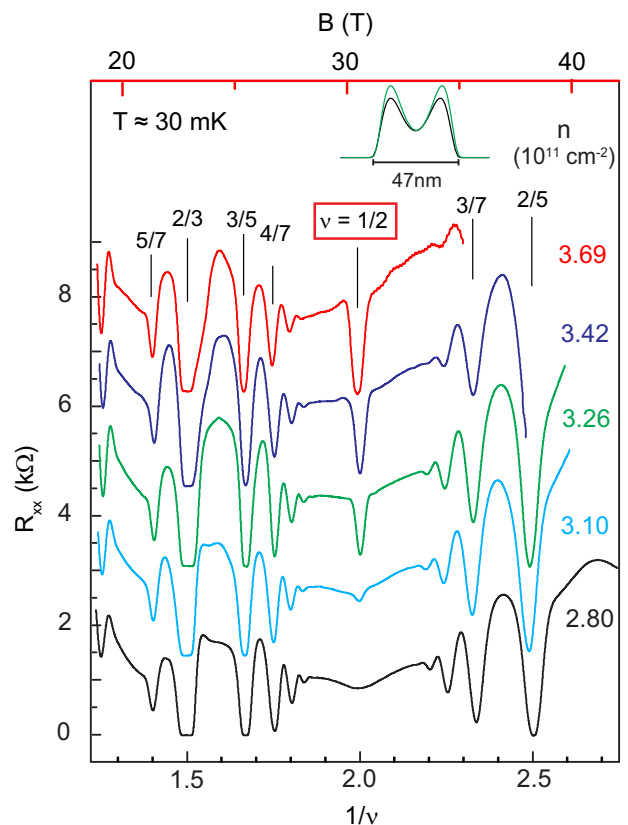


FIG. 2. (color online) R_{xx} plotted vs inverse filling factor for the 47-nm-wide QW for different densities. All traces were taken for symmetric total charge distributions ("balanced" QW). Except for the lowest density, the traces are offset vertically for clarity. In each trace, $R_{xx} \simeq 0$ at $\nu = 2/3$. The inset shows the calculated charge distributions for $n = 2.80$ (black) and $3.26 \times 10^{11} \text{ cm}^{-2}$ (green). The top axis is the perpendicular magnetic field for the $n = 3.69 \times 10^{11} \text{ cm}^{-2}$ (red) trace; note that R_{xx} at $\nu = 1/2$ essentially vanishes in this trace.

FQHE at $\nu = 1/2$. As the density increases, the traces reveal a clear sharp minimum developing in R_{xx} at $\nu = 1/2$ which is accompanied by a quantized plateau in R_{xy} at $2h/e^2$. In the inset we show the calculated charge distributions for $n = 2.80 \times 10^{11} \text{ cm}^{-2}$ (black), when the state at $\nu = 1/2$ is compressible, and $n = 3.26 \times 10^{11} \text{ cm}^{-2}$ (green), when the $\nu = 1/2$ FQHE is observed. It is clear that a very small change in the charge distribution is sufficient to turn the ground state at $\nu = 1/2$ from compressible to FQHE.

Similar data for a slightly narrower, 46-nm-wide QW are shown in Fig. 3. The data again attest to the very high quality of this sample, as they exhibit high-order FQHE at odd-denominator fillings up to $7/15$ and $8/15$. The trend for the ground state at $\nu = 1/2$ is similar to the 47-nm-wide sample of Fig. 2: At the lowest density the state is compressible but as the density is slightly increased a FQHE appears. But note in Fig. 3 that the

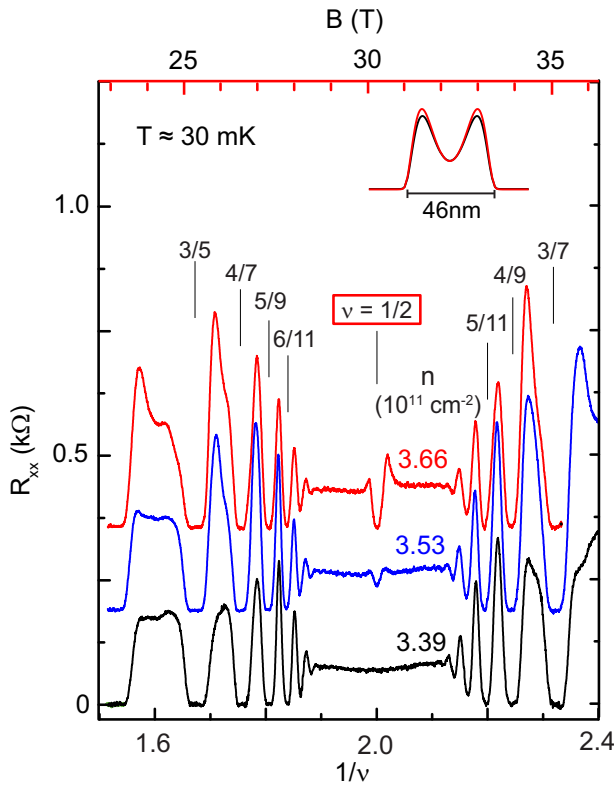


FIG. 3. (color online) R_{xx} plotted vs inverse filling factor for the 46-nm-wide QW for different densities while the total charge distribution was kept symmetric. The upper two traces are shifted vertically for clarity. The inset shows the calculated charge distributions for $n = 3.39$ (black) and $3.66 \times 10^{11} \text{ cm}^{-2}$ (red). The top axis is the perpendicular magnetic field for the $n = 3.66 \times 10^{11} \text{ cm}^{-2}$ trace.

density for the transition between the compressible and FQHE ground state is somewhat larger for the 46-nm-wide sample compared to the slightly wider QW of Fig. 2.

We have made measurements similar to those shown in Figs. 2 and 3 for several samples with different QW widths, and summarize the results in various "phase diagrams" shown in Figs. 4-6. In these figures, filled symbols indicate that the $\nu = 1/2$ FQHE is stable. The size of the filled symbols for data from some representative QW widths ($W = 46, 47, 56,$ and 77 nm) give an approximate indication of the strength of the FQHE as deduced, e.g., from the depth of the $\nu = 1/2$ R_{xx} minimum or from the measured energy gaps [24, 25]. The open symbols in Figs. 4-6 denote the absence of a $\nu = 1/2$ FQHE. In all the samples, the trend is the same: The $\nu = 1/2$ FQHE is seen in an intermediate density range which depends on the QW width, but turns into a compressible state when the density is sufficiently lowered. In Figs. 4-6 we mark the approximate boundary between the FQHE and the compressible state with a dashed curve. This boundary is the main focus of our work presented here.

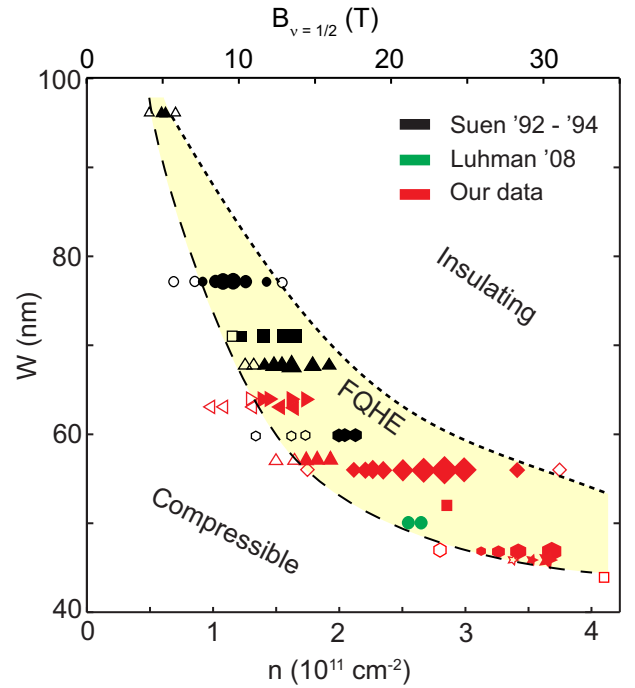


FIG. 4. (color online) The well-width (W) vs density (n) phase diagram for the state of the electron system at $\nu = 1/2$ in wide GaAs QWs. Filled symbols represent the presence of a $\nu = 1/2$ FQHE and open symbols its absence. Data points in black are from Refs. [22–25] and those in green from Ref. [29].

Note also that at sufficiently high densities, the electron system turns into an insulating phase whose characteristics suggest the formation of a pinned bilayer Wigner crystal [26]. We have indicated the boundary between the FQHE and the insulating phase with a dotted curve in Figs. 4-6. This boundary, and the properties of the insulating phase are interesting in their own right, but are beyond the scope of our study [33].

The phase diagrams in Figs. 4-6 provide different perspectives on the stability of the $\nu = 1/2$ FQHE in wide GaAs QWs. Figure 4 provides the simplest phase diagram for the $\nu = 1/2$ FQHE stability in a wide QW as it gives the range of densities within which the $1/2$ FQHE is observed in a GaAs QW of width W [34]. It is clear that the narrower the QW, the higher the density range where the $\nu = 1/2$ FQHE is stable. In Fig. 4 it also appears that there is a discrepancy between the old data (black symbols) of Suen *et al.* [22–25] and the new data for the narrower QWs (red symbols) in terms of the boundary separating the FQHE and compressible phases. The origin of this discrepancy is not entirely clear, but it may stem from the following differences between the two sets of samples. First, the mobilities of the older samples are about a factor of three lower than the mobilities of the new samples; this may have hindered the observation of the $\nu = 1/2$ FQHE at lower densities in the old samples.

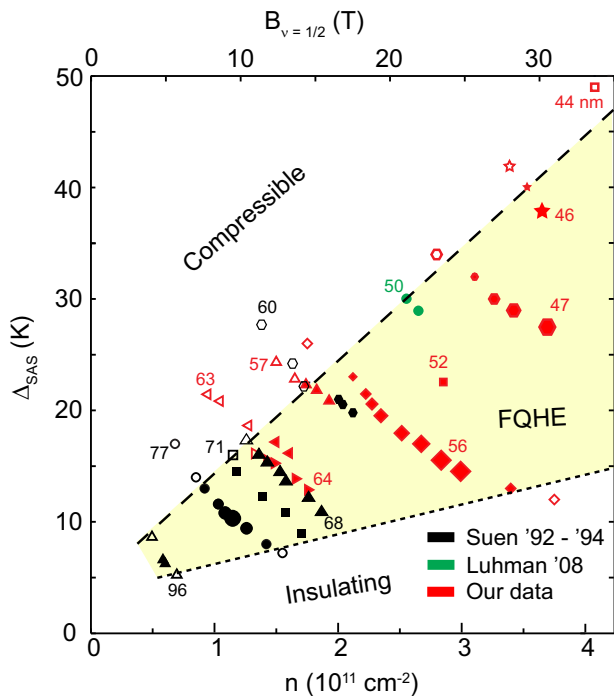


FIG. 5. (color online) Experimentally measured subband separation energy (Δ_{SAS}) is plotted as a function of density (n) for electron systems confined to wide GaAs QWs. The symbols have the same meaning as in Fig. 4, and the well width is given (in units of nm) next to each set of data points. Note that the boundary between the FQHE and compressible states appears to be a *straight* line (dashed line) over the entire range of QW widths and densities in our study.

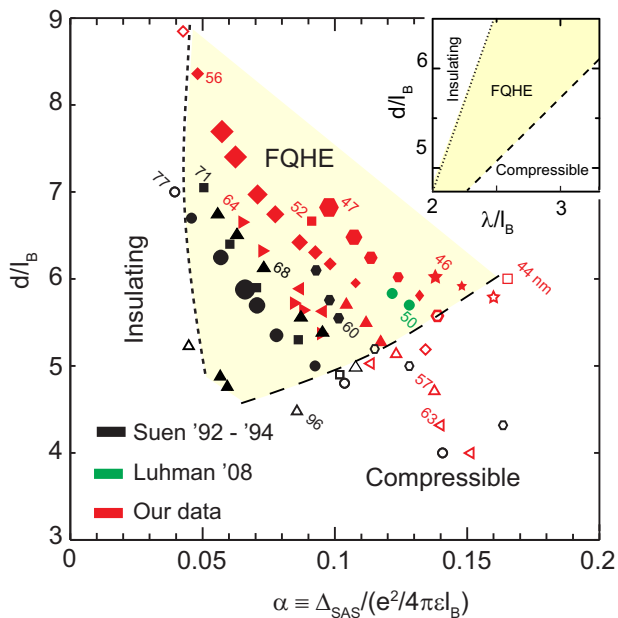


FIG. 6. (color online) The d/l_B vs $\alpha = \Delta_{SAS}/(e^2/4\pi\epsilon l_B)$ phase diagram for the observation of the $\nu = 1/2$ FQHE in wide GaAs QWs. The well widths are given in units of nm. The upper-right inset shows a d/l_B vs λ/l_B phase diagram.

Second, the older samples had somewhat larger barrier heights (Al composition $x \simeq 0.30$) compared to the new samples ($x \simeq 0.24$). This makes the older samples effectively narrower relative to the new samples as it raises Δ_{SAS} and reduces the inter-layer separation for a given QW width and density. Third, the self-consistent calculations, which were used to fit the Δ_{SAS} vs n data and extract values of W , were different and used slightly different band parameters [35]. We believe that the latter two factors, and not the mobility difference, are responsible for the discrepancy between the old and new sets of data in Fig. 4 phase diagram. As seen in the phase diagram of Fig. 5 where the *measured* values of density and Δ_{SAS} are plotted, this discrepancy indeed disappears, and the boundary separating the FQHE and compressible states at $\nu = 1/2$ is described by one curve (a simple line) for all the samples [36]. We reiterate that our overall estimated accuracy for the quoted W is about $\pm 5\%$.

Figure 5 gives one of the relevant energy scales for the $\nu = 1/2$ FQHE stability. Here we plot the measured values of Δ_{SAS} vs n . As clearly seen in this plot, for a given QW width, Δ_{SAS} decreases as n is increased. The plot of Fig. 5 demonstrates that at the boundary between the compressible and FQHE states Δ_{SAS} is larger for larger densities. More remarkably, this boundary appears to be well described by essentially a *straight* line (dashed line in Fig. 5). We are not aware of any theoretical calculations which predict such a simple (linear) boundary for the transition between the compressible and FQHE phases in wide QWs.

Finally, we provide the phase diagram of Fig. 6 which is often used to discuss the origin and stability of the $\nu = 1/2$ FQHE in a wide QW or in a double QW system [14, 19, 24, 25]. This diagram takes into account the competition between three relevant energies [37]: (i) the inter-layer tunneling energy (Δ_{SAS}), (ii) the intra-layer (in-plane) Coulomb energy ($e^2/4\pi\epsilon l_B$), and (iii) the inter-layer Coulomb energy ($e^2/4\pi\epsilon d$). The coordinates in the diagram of Fig. 6 are the ratios of $\Delta_{SAS}/(e^2/4\pi\epsilon l_B)$, which we denote as α , and $(e^2/4\pi\epsilon l_B)/(e^2/4\pi\epsilon d)$ which is equal to d/l_B . Note that in a wide QW, as the density increases, α decreases because both Δ_{SAS} and l_B (at $\nu = 1/2$) decrease, and d increases.

In Fig. 6, when $\alpha = 0$ and $d/l_B > 0$, the electrons are in a bilayer system with zero tunneling. If d/l_B is very large, there should be no FQHE at $\nu = 1/2$ as the electron system behaves as two independent layers with little or no inter-layer interaction, each at filling factor $\nu = 1/4$. As the layers are brought closer together ($d/l_B \lesssim 2$), a $\nu = 1/2$ FQHE, described by the two-component Ψ_{331} state, is possible. This is indeed believed to be the case for the $\nu = 1/2$ FQHE observed in bilayer electron systems in double QW samples with very little inter-layer tunneling [14, 21, 38]. For finite values of tunneling ($\alpha > 0$) two types of FQHE states can exist at $\nu = 1/2$. At small values of α the intra-layer

correlations can dwarf the tunneling energy, thus stabilizing a two-component Ψ_{331} FQHE state. At larger α , on the other hand, the one-component (Pfaffian) FQHE might be stable. For very large α , it is most likely that the ground state is compressible. The relative stabilities of a $\nu = 1/2$ Ψ_{331} or Pfaffian FQHE state compared to a compressible state are of course also influenced by the inter-layer to intra-layer interactions (d/l_B) as well as the thickness of the "layers" (the parameter λ in Fig. 1 and Fig. 6 insets), which softens the intra-layer short-range interactions [22, 25].

Following some of the earlier theoretical work [7–15], recently there have been several reports of calculations to determine the stability of the different FQHE and compressible states in double and wide QWs [16–20]. A main conclusion of these calculations is that the Pfaffian FQHE state at $\nu = 1/2$ is not stable in a strictly 2D electron system with zero layer thickness [18]. However, for a system with finite (non-zero) layer thickness and tunneling, such as electrons in a wide QW, the calculations indicate that at $\nu = 1/2$ the Pfaffian FQHE state could in principle exist at relatively large values of α . In particular, the Ψ_{331} FQHE state is found to be stable in a range of small values of α but as α increases the system makes a transition into a Pfaffian state before it becomes compressible at very large values of α [16, 19]. Interestingly, the calculations suggest that very near the transition between the Ψ_{331} and Pfaffian states, the energy gap for the $1/2$ FQHE is a maximum, i.e., there is an upward cusp in the energy gap vs α plot [16, 19]. This is indeed what is qualitatively seen in experiments [24, 25]. In Ref. [16] it was concluded that the presence of this cusp and the finite value of the energy gap on the Pfaffian side suggest that the Pfaffian state could be stable at $\nu = 1/2$ in wide QWs. Authors of Ref. [19], on the other hand, concluded that although a Pfaffian FQHE state at $\nu = 1/2$ could in principle exist near this cusp, the chances that such a state would survive in the thermodynamic limit are slim [18].

The phase diagrams we present here provide the comprehensive experimental conditions under which the $\nu = 1/2$ FQHE is observed in wide GaAs QWs with symmetric charge distributions. We note that the samples whose data we summarize in these diagrams span a large parameter range (well width, density, mobility), and yet the observed trends are remarkably consistent among the different samples. Of special interest are the samples with relatively narrow QW width, i.e., with large α where the Pfaffian state is most likely to exist. We would like to emphasize that in the phase diagram of Fig. 6, α for our narrowest QW ($W = 46$ nm) in which we observe the $\nu = 1/2$ FQHE is $\simeq 0.15$. This is the largest α at which a FQHE at $\nu = 1/2$ has been observed, and exceeds typical values of α where the Ψ_{331} is theoretically predicted to be stable [19].

We close by drawing two conclusions. First, we empha-

size that all the data presented here were taken on wide GaAs QWs whose total charge distributions were symmetric ("balanced"). It has been experimentally demonstrated that even small amounts of charge distribution asymmetry ($\simeq 5\%$) cause a destruction of the $\nu = 1/2$ FQHE and a transition into a compressible state [24–28, 30]. This trend continues in the narrowest QWs where we have seen a $\nu = 1/2$ FQHE; e.g., in the 46-nm-wide QW at $n = 3.53 \times 10^{11}$ cm $^{-2}$, a charge imbalance of 5% causes a collapse of the $\nu = 1/2$ FQHE and a compressible state appears. Concurring with the conclusion reached in previous experimental studies [24–27, 30], we suggest that the $\nu = 1/2$ FQHE observed in symmetric, wide GaAs QWs is a two-component state, stabilized by a delicate balance between the intra-layer and inter-layer correlations [38].

It is worth noting that the two-component Ψ_{331} state is theoretically expected to be stable when the intra-layer and inter-layer Coulomb interactions are comparable, i.e., have a ratio of about unity [10, 12]. For an ideal bilayer electron system (with zero layer thickness), the ratio d/l_B accurately reflects the relative strengths of the intra-layer and inter-layer Coulomb interactions and the $\nu = 1/2$ FQHE should be observable for $d/l_B \lesssim 2$. However, in an electron system whose layer thickness is comparable to or larger than l_B , the short-range component of the Coulomb interaction, which is responsible for the FQHE, softens [40, 41]. This softening is significant in bilayer electron systems confined to wide QWs and, in particular, λ/l_B (for each layer) is about 2.3 to 3.3 in the regime where the $\nu = 1/2$ FQHE is stable (see Fig. 6 inset) [22–25]. Associating the $\nu = 1/2$ FQHE we observe with the Ψ_{331} state, it is thus not surprising that we see this FQHE when d/l_B is much larger than unity (Fig. 6): The short-range component of the intra-layer interaction is weaker for a bilayer system with larger λ/l_B ; therefore to ensure the proper intra-layer to inter-layer interaction ratio which favors the Ψ_{331} state, a relatively weaker inter-layer interaction (smaller $e^2/4\pi\epsilon d$) is also needed, implying a larger d/l_B [25]. It is clearly evident in Fig. 6 inset that for a sample with larger λ/l_B , the $\nu = 1/2$ FQHE is stable in a region of larger d/l_B [24, 25].

Second, the experimental boundaries we have determined experimentally (Figs. 4–6) should provide incentive for future theoretical work. For example, the fact that the boundary between the FQHE and compressible state in Fig. 5 (dashed line) is essentially a straight line is intriguing. Moreover, the same boundary in the d/l_B vs α diagram of Fig. 6 is nearly horizontal and suggests that the critical d/l_B values for the transition are between $\simeq 4.5$ and 6.0 in the range of $0.05 < \alpha < 0.15$ [39]. This is very different from the relevant boundaries obtained in calculations. For example, the boundary calculated in Ref. [19] for the stability of the Ψ_{331} FQHE state has a much stronger dependence on α . We conclude that, in light of our new data, more detailed and precise calcu-

lations are needed to make a quantitative connection to the experimental data and help unveil the origin of the $\nu = 1/2$ FQHE in symmetric, wide GaAs QWs.

We acknowledge support through the Keck Foundation, the Moore Foundation, and the National Science Foundation (grants DMR-0904117, DMR-1305691, and MRSEC DMR-0819860). A portion of this work was performed at the National High Magnetic Field Laboratory which is supported by National Science Foundation Cooperative Agreement No. DMR-1157490, the State of Florida and the US Department of Energy. We are grateful to J.K. Jain and Z. Papić for illuminating discussions, and to E. Palm, S. Hannahs, T. P. Murphy, J. H. Park and G. E. Jones for technical assistance with the high magnetic field measurements.

-
- [1] D. C. Tsui, H. L. Stormer, and A. C. Gossard, *Phys. Rev. Lett.* **48**, 1559 (1982).
- [2] J. K. Jain, *Composite Fermions* (Cambridge University Press, Cambridge, UK, 2007).
- [3] R. L. Willett, J. P. Eisenstein, H. L. Stormer, D. C. Tsui, A. C. Gossard, and J. H. English, *Phys. Rev. Lett.* **59**, 1776 (1987).
- [4] W. Pan, J.-S. Xia, V. Shvarts, D. E. Adams, H. L. Stormer, D. C. Tsui, L. N. Pfeiffer, K. W. Baldwin, and K. W. West, *Phys. Rev. Lett.* **83**, 3530 (1999).
- [5] C. Nayak, S. H. Simon, A. Stern, M. Freedman, and S. Das Sarma, *Rev. Mod. Phys.* **80**, 1083 (2008).
- [6] B. Halperin, *Helv. Phys. Acta* **56**, 75 (1983).
- [7] G. Moore and N. Read, *Nuclear Physics B* **360**, 362 (1991).
- [8] E. H. Rezayi and F. D. M. Haldane, *Bull. Am. Phys. Soc.* **32**, 892 (1987).
- [9] T. Chakraborty and P. Pietiläinen, *Phys. Rev. Lett.* **59**, 2784 (1987).
- [10] D. Yoshioka, A. H. MacDonald, and S. M. Girvin, *Phys. Rev. B* **39**, 1932 (1989).
- [11] A. MacDonald, *Surf. Sci.* **229**, 1 (1990).
- [12] S. He, X. C. Xie, S. Das Sarma, and F. C. Zhang, *Phys. Rev. B* **43**, 9339 (1991).
- [13] M. Greiter, X.-G. Wen, and F. Wilczek, *Phys. Rev. Lett.* **66**, 3205 (1991).
- [14] S. He, S. Das Sarma, and X. C. Xie, *Phys. Rev. B* **47**, 4394 (1993).
- [15] B. I. Halperin, *Surf. Sci.* **305**, 1 (1994).
- [16] K. Nomura and D. Yoshioka, *J. Phys. Soc. of Jap.* **73**, 2612 (2004).
- [17] Z. Papić, N. Regnault, and S. Das Sarma, *Phys. Rev. B* **80**, 201303 (2009).
- [18] M. Storni, R. H. Morf, and S. Das Sarma, *Phys. Rev. Lett.* **104**, 076803 (2010).
- [19] M. R. Peterson and S. Das Sarma, *Phys. Rev. B* **81**, 165304 (2010).
- [20] M. R. Peterson, Z. Papić, and S. Das Sarma, *Phys. Rev. B* **82**, 235312 (2010).
- [21] J. P. Eisenstein, G. S. Boebinger, L. N. Pfeiffer, K. W. West, and S. He, *Phys. Rev. Lett.* **68**, 1383 (1992).
- [22] Y. W. Suen, L. W. Engel, M. B. Santos, M. Shayegan, and D. C. Tsui, *Phys. Rev. Lett.* **68**, 1379 (1992).
- [23] Y. W. Suen, M. B. Santos, and M. Shayegan, *Phys. Rev. Lett.* **69**, 3551 (1992).
- [24] Y. W. Suen, Ph.D. thesis, Princeton University (1993).
- [25] Y. W. Suen, H. C. Manoharan, X. Ying, M. B. Santos, and M. Shayegan, *Phys. Rev. Lett.* **72**, 3405 (1994).
- [26] H. C. Manoharan, Y. W. Suen, M. B. Santos, and M. Shayegan, *Phys. Rev. Lett.* **77**, 1813 (1996).
- [27] M. Shayegan, H. C. Manoharan, Y. W. Suen, T. S. Lay, and M. B. Santos, *Semiconductor Science and Technology* **11**, 1539 (1996).
- [28] M. Shayegan, in *Topological Aspects of Low Dimensional Systems*, edited by A. C. A. Comtet, T. Jolicœur, and S. Ouvry (Springer, Berlin, 1999), pp. 1–51.
- [29] D. R. Luhman, W. Pan, D. C. Tsui, L. N. Pfeiffer, K. W. Baldwin, and K. W. West, *Phys. Rev. Lett.* **101**, 266804 (2008).
- [30] J. Shabani, T. Gokmen, and M. Shayegan, *Phys. Rev. Lett.* **103**, 046805 (2009).
- [31] J. Shabani, T. Gokmen, Y. T. Chiu, and M. Shayegan, *Phys. Rev. Lett.* **103**, 256802 (2009).
- [32] Y. W. Suen, J. Jo, M. B. Santos, L. W. Engel, S. W. Hwang, and M. Shayegan, *Phys. Rev. B* **44**, 5947 (1991).
- [33] The dotted boundary in Figs. 4-6 is difficult to determine in narrower QWs because of the very high densities, and hence very high magnetic fields, that are required for its access.
- [34] In Ref. [23] a value of 80 nm was quoted for the sample QW width but, as discussed in Ref. [24], subsequent studies indicated that the width is closer to 77 nm. In Figs. 4-6 we are not including data from Ref. [23] because their data in fact closely overlap with the data presented in Ref. [25] which were taken on another 77-nm-wide QW from a different wafer.
- [35] The values of W we give here for the old samples are those quoted in Refs. [24, 25].
- [36] Note in Fig. 5 that the measured Δ_{SAS} values for the old, 60-nm-wide QW are very similar to those for the slightly narrower (57-nm-wide) new QW; similarly, the old 68-nm-wide sample's Δ_{SAS} are very close to the 64-nm-wide QW sample.
- [37] A fourth relevant energy is the Zeeman energy $E_Z = [g^* \mu_B B]$ where g^* is the effective Lande g -factor and μ_B is the Bohr magneton. Using the GaAs band value of $g^* = -0.44$, $E_Z = 0.3$ K/T. This is smaller than Δ_{SAS} at magnetic fields where the $\nu = 1/2$ FQHE is observed in our samples (see, e.g., Fig. 5), implying that the spin degree of freedom is important. However, in our wide GaAs QW samples, g^* is typically enhanced by a factor of $\simeq 10$ or larger [43], so that E_Z is more than twice larger than Δ_{SAS} . We therefore expect the spin degree of freedom not to play a role in the stability of the $\nu = 1/2$ FQHE in our samples. This is consistent with data in tilted magnetic field data which show that, starting near the compressible-FQHE boundary, the $\nu = 1/2$ FQHE gets stronger at small tilt angles [29, 44]. Such strengthening is consistent with Δ_{SAS} becoming effectively smaller because of the parallel field component [45], thus moving the electron system towards a region of higher stability for the FQHE (see, e.g., Fig. 5).
- [38] It is worth emphasizing that the experimental phase diagram we present in Fig. 6 is for electron systems confined to a *single wide* GaAs QWs. The data of Ref. [21], which

exhibit $\nu = 1/2$ FQHE in *double* GaAs QWs with very small inter-layer tunneling ($\alpha \simeq 0.01$) and $d/l_B \simeq 2$, fall well outside the yellow-shaded region of Fig. 6 where the $1/2$ FQHE is stable in wide GaAs QWs. An intriguing question is how far would the yellow region in Fig. 6 extend for even wider GaAs QWs, and whether it would ever contain the parameter range where the $1/2$ FQHE is stable in double QWs.

- [39] The observation of developing FQHE states in highly asymmetric, wide GaAs QWs near fillings factors $\nu = 1/2$ and $1/4$ was recently reported and was interpreted to suggest that these states might have a one-component origin [31]. Subsequent calculations, however, seem to indicate that these are more likely two-component states, stabilized by a partial subband polarization [46].
- [40] M. Shayegan, J. Jo, Y. W. Suen, M. Santos, and V. J. Goldman, Phys. Rev. Lett. **65**, 2916 (1990).
- [41] S. He, F. C. Zhang, X. C. Xie, and S. Das Sarma, Phys. Rev. B **42**, 11376 (1990).
- [42] It is worth noting that the value of W/l_B at the compressible-FQHE boundary is also nearly a constant and ranges between 8.0 and 9.5.
- [43] Yang Liu, J. Shabani, and M. Shayegan, Phys. Rev. B **84**, 195303 (2011).
- [44] T. S. Lay, T. Jungwirth, L. Smrčka, and M. Shayegan, Phys. Rev. B **56**, R7092 (1997).
- [45] J. Hu and A. H. MacDonald, Phys. Rev. B **46**, 12554 (1992).
- [46] V. W. Scarola, C. May, M. R. Peterson, and M. Troyer, Phys. Rev. B **82**, 121304 (2010).